WILEY-VCH

FULL PAPER

Correlation between ionic liquid cytotoxicity and liposome-ionic liquid interactions

Suvi-Katriina Ruokonen,[a] Corinna Sanwald,[b] Alexandra Robciuc,[c] Sami Hietala,[a] Antti H. Rantamäki,[a] Joanna Witos,[a] Alistair W.T. King,[a] Michael Lämmerhofer,[b] and Susanne K. Wiedmer*[a]

Abstract: This study aims at extending the understanding of the toxicity mechanism of ionic liquids (ILs) using various analytical methods and cytotoxicity assays. The cytotoxicity of eight ILs and one zwitterionic compound was determined using mammalian and bacterial cells. The time dependency of the IL toxicity was assessed using human corneal epithelial cells. Hemolysis was performed using human red blood cells and the results were compared with destabilization data of synthetic liposomes upon addition of ILs. The effect of the ILs on the size and zeta potential of liposomes revealed information on changes in the lipid bilayer. Differential scanning calorimetry was used to study the penetration of the ILs into the lipid bilayer. Pulsed field gradient nuclear magnetic resonance spectroscopy was used to determine whether the ILs occurred as unimers, micelles, or if they were bound to liposomes. The results show that the investigated ILs can be divided into three groups based on the cytotoxicity mechanism: cell wall disrupting ILs, ILs exerting toxicity through both cell wall penetration and metabolic alteration, and ILs affecting solely cell metabolism.

Introduction

Ionic liquids (ILs; Figure 1) are commonly defined as liquid organic salts, consisting of an anion and a cation and having melting points below 100 °C. ILs are often quoted as designer solvents because the selection of an appropriate IL cation and anion pair allows the generation of ILs with a diversity of physical and chemical properties. Owing to their unique properties, ILs are a commonly used organic salt group in various industrial, commercial, and pharmaceutical applications. Several of these applications such as their usage in pharmaceutical[1], environmental[2], and in food[3] related applications, in organic synthesis and catalysis[4], and in analytical chemistry[5] have been reviewed previously.

ILs are often claimed as “green” due to their “nonflammable” nature and low vapor pressure. Hence, their evaporation into the atmosphere is miniscule and requires a vast amount of energy. However, many classes of ILs are water-soluble and they can end up into the aqueous ecosystem through accidental spills and drains. Moreover, due to the high variety of possible IL combinations not all ILs are biodegradable and they can bioaccumulate into small aquatic organisms and furthermore be transferred to animals in higher trophic levels in a food chain, and eventually even to humans.

There are a myriad of studies regarding IL toxicity[6], yet, due to the structural variety of ILs, the mechanism of toxicity is still poorly known. The cation and anion selection, alkyl chain length, and the oxygenated functional groups are few properties known to affect the toxicity of ILs. In addition to the IL properties, the test organism and the IL environment (solvent, pH, temperature etc.) influence the observed results. Toxicity measurements, which best describe the harmfulness to humans, such as animal tests using rats, fish etc. are usually expensive, time consuming, and ethically dubious. Herein, the purpose was to gain more information on the IL cytotoxicity. In addition, we wanted to investigate if it is possible to obtain similar information with novel analytical methodologies without the use of living organisms. Because the plasma membrane is the first cellular constituent encountered by an external toxicant, *i.e.* the IL, biomimetic phospholipid membranes (liposomes) were used as target objects for this purpose. Large unilamellar liposomes (LUV), consisting of phospholipid bilayers enclosing an aqueous compartment, are excellent models for the cell membranes. The possibility to modify the amount and quality of the membrane building blocks (phospholipids, cholesterol, sugars, proteins etc.) is also a great advantage of using liposomes.

The intercalation properties of surface-active ILs into cell membranes are known to affect the toxicity of ILs and hence, the IL-cell membrane interactions are widely studied by utilizing liposomes.[7] The interdependency of hydrophobicity and toxicity of ILs is generally supported in many such publications.[8] The toxicity of surface-active ILs is speculated to be due to a facilitated uptake of a compound into an organism, leading to an increased internal toxicant concentration and to an altered metabolism. Another hypothesis is that IL-induced perturbation and increase of the membrane fluidity might result in alterations of the ion and/or molecule transport through the membrane.[9] Yet, it is clear that the toxicity increases when adsorbed or absorbed

[a] S.-K. Ruokonen, Dr. S. Hietala, Dr. A.H. Rantamäki, Dr. J. Witos, Dr. A.W.T. King, Dr. S.K. Wiedmer
Department of Chemistry
Faculty of Science, University of Helsinki
A.I. Virtasen aukio 1, 00560 Helsinki, Finland
E-mail: Susanne.wiedmer@helsinki.fi
[b] C. Sanwald, Prof. Dr. M. Lämmerhofer
Institute of Pharmaceutical Sciences, University of Tübingen
Auf der Morgenstelle 8, 72076, Tübingen, Germany
[c] Dr. A. Robciuc
Helsinki Eye Lab, Ophthalmology
University of Helsinki and Helsinki University Hospital
Haartmaninkatu 8, 00290, Helsinki, Finland

Supporting information, containing calculations of HCE lipid concentration and amount and surface area of liposomes, figure on size distribution of liposomes, and IL synthesis and characterization, of this article can be found under XXX.

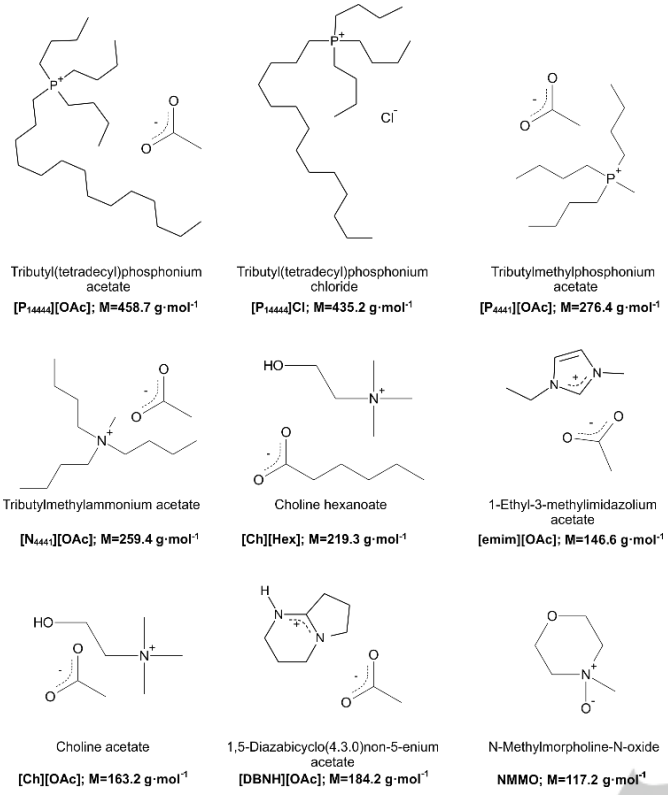

Figure 1. Structures of the studied compounds.

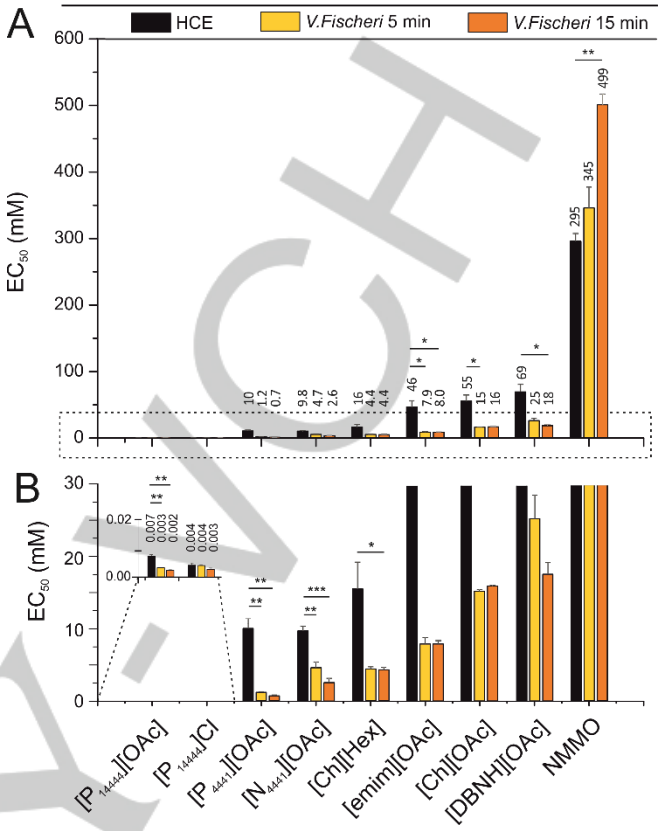

Figure 2. A) Median effective concentrations (EC_{50}) of ILs and NMMO determined using HCE and *V. fischeri* cells. B) Magnification of figure A. One-way ANOVA with Tukey HSD post-hoc test, ***p<0.001, **p<0.01, and *p<0.05. n=5,2,2; 5,2,2; 3,2,2; 3,6,5; 3,2,3; 3,2,2; 4,2,2; 3,2,2; and 3,3,2 for the compounds from left to right.

hydrophobic ILs compromise the membrane integrity. Surface-active ILs have been speculated to permeate into the membrane inducing roughening[10] and/or swelling[8c] of the membrane prior to membrane leakage and/or even membrane disruption. Lipids, disengaged from the disrupted liposomes, have further been shown to aggregate with surface-active imidazolium based ILs forming IL-lipid micelles,[8c] as seen also with other surfactants.[11] In addition, imidazolium and cholinium based ILs with lactate anion[12] and imidazolium, pyrrolidinium, and pyridinium based ILs[7a] have been shown to even induce liposome fusion.

In this study, our aim was to deepen the knowledge of the IL toxicity mechanism utilizing various analytical methods and comparing these results with data obtained from cytotoxicity measurements.

Results and Discussion

Cytotoxicity of ILs toward human corneal epithelial and Vibrio fischeri cells

To evaluate the toxicity of the ILs, the median effective concentration (EC_{50}) were determined using human corneal epithelial (HCE) cells and *Vibrio fischeri* (*V. fischeri)* bacteria. Moreover, the EC_{50} values shown in Figure 2 and summarized in Table 1 were utilized in the selection of appropriate IL concentrations for the liposome studies.

Tributyl(tetradecyl)phosphonium acetate ([P_{14444}][OAc]) and tributyl(tetradecyl)phosphonium chloride ([P_{14444}]Cl) were the most toxic ILs and based on a classification system introduced in our previous study,[13] they were classified as “toxic”. Methyltributylphosphonium acetate ([P_{4441}][OAc]) and methyltributylammonium acetate ([N_{4441}][OAc]) were classified as “practically harmless” or “harmless” and the rest of the compounds, *i.e.,* 1-ethyl-3-methylimidazolium acetate ([emim][OAc]), 1,5-diazabicyclo(4.3.0)non-5-enium acetate ([DBNH][OAc]), choline hexanoate ([Ch][Hex]), choline acetate ([Ch][OAc]), and *N*-methylmorpholine-*N*-oxide (NMMO) were classified as “harmless”. The results are in a good agreement with the afore mentioned study where the EC_{50} values of [P_{14444}][OAc], [P_{4441}][OAc], [emim][OAc], and [DBNH][OAc] were determined.[13] All compounds, excluding [P_{14444}]Cl and NMMO, were significantly ($p < 0.05$, One-way ANOVA with Tukey HSD post-hoc test) more toxic toward the bacteria than toward the HCE cells, which is consistent with previous studies where cytotoxicities of ILs[6a] and energetic compounds[14] were assessed using different mammalian and bacterial cell lines. This and the difference in the incubation times of HCE and *V. fischeri* cells (24 hours and 15 minutes, respectively) indicate that the mammalian cells were more resistant toward the external toxicants. The difference can

Table 1. Summary of results: EC_{50} values and effect of time on cytotoxicity . Effect of analytes on hemolysis and on size, zeta potential, and transition temperaturre of liposomes. Diffusion constants with liposomes.

	Cytotoxicity (EC_{50} in mM)			Time dependency	Hemolysis	Zetasizer		DSC	NMR			
					Concentration range [effective concentration] (mM)							
	HCE cells	*V.Fischeri* 5 min	*V.Fischeri* 15 min	Cell death reached (hours) [Cell death %]	[Lysis]	Size [disruption of liposomes]	zeta potential [potential conversion]	[T_m change]	Concentration range (mM)	D_{Cation} (10^{-10} $m^2 \cdot s^{-1}$)	D_{Anion} (10^{-10} $m^2 \cdot s^{-1}$)	CMC in water (mM)
[P_{14444}][OAc]	0.0071 ± 0.0005	0.0031 ± 0.0002	0.0022 ± 0.0002	≤2 [40]	0.0007-0.044 [0.011]	0-1 [1]	0-0.8 [0.015]	0-5 [0.01]	0.5 - 5	0.1 - 0.6	5.8 - 7.1	0.89 ± 0.01
[P_{14444}][Cl]	0.0041 ± 0.0006	0.0039 ± 0.0000	0.0027 ± 0.0004	≤2 [40]	0.0007-0.046 [0.0115]	0-1 [1]	0-0.8 [0.015]	0-5 [0.01]	0.5-6	0.1 - 0.6	5.8 - 7.1	1.0
[P_{4441}][OAc]	10 ± 1.3	1.2 ± 0.1	0.67 ± 0.12	8–24 [40]	0.7-45 [n/a]	0-30	0-25	0-180 [10]	1 - 30	3.5 - 3.6	6.5 - 6.7	297 ± 11
[N_{4441}][Oac]	9.8 ± 0.7	4.7 ± 0.8	2.6 ± 0.6	8–24 [15]	0.75-48 [n/a]	0-30	0-25	0-180 [100]	3 - 40	3.4 - 3.7	6.5 - 6.8	
[Ch][Hex]	16 ± 3.7	4.4 ± 0.3	4.3 ± 0.4	8–24 [25]	3.6-228 [n/a]	0-50	0-50	0-200 [15]	1 - 50	6.2 -6.4	4.5 - 4.8	673 ± 2
[emim][OAc]	46 ± 9.3	7.9 ± 0.9	8.0 ± 0.5	8–24 [25]	2.3-147 [n/a]	0-120	0-60	0-300 [n/a]	1 - 70	6.2 - 6.3	6.6 - 6.9	nd
[Ch][OAc]	55 ± 9.0	15 ± 0.2	16 ± 0.2	8–24 [25]	4.8-306 [n/a]	0-100	0-50	0-300 [n/a]	3 - 150	6.2 - 6.5	6.5 - 6.9	nd
[DBNH][OAc]	69 ± 11	25 ± 3.3	18 ± 1.6	8–24 [25]	4.2-271 [n/a]	0-100	0-40	0-400 [n/a]	1 - 200	5.2 - 5.5	6.2 - 6.6	nd
NMMO	295 ± 11	345 ± 31	499 ± 16	8–24 [40]	13.3-850 [n/a]	0-420	0-420	0-800 [200]	5 - 500	4.7 - 5.2		nd

n/a no effect; D diffusion constant; nd not detected

be explained by the variation in the cell structure and metabolism of the prokaryotic and eukaryotic cells. Another plausible explanation is the difference in the EC_{50} determination methods of the assays. Whereas the metabolically active alamarBlue dye is reduced in the presence of living HCE cells, the decay in the bioluminescence of the *V. fischeri* bacteria is recorded. In short, the bioluminescence arises when luciferin is oxidized with a help of luciferase enzyme. Therefore, the bioluminescence inhibition is not necessarily solely affected by cell death, but can occur when the gene expression or energy transfer processes *etc.* of the bacteria are altered.[15] Mariscal *et al.* have shown that the bioluminescence of *Vibrio harveyi* increased when they were exposed to organic solvents, known to permeate the bacteria membrane, at concentrations below their toxic ranges.[16] The bioluminescence might therefore even increase after the bacteria have adjusted to the external permeating substance, *i.e.* NMMO. This seems especially likely for substances which are only slightly toxic or non-toxic, *i.e.,* are not lethal to the bacteria within the time period the bioluminescence is recorded. For instance, the EC_{50} value of NMMO was lower when HCE cells were used instead of *V. fischeri* bacteria indicating that after the initial 'shock' caused by the addition of NMMO to the bacteria the bioluminescence increased as a function of time. In order to gain more information on the time dependency of the toxicity of ILs, a real-time cytotoxicity assay was performed.

Real-time cytotoxicity assay

The EC_{50} value measurements showed that the ILs are cytotoxic over a relatively wide range of concentrations. To gain more insight into this process, a CellTox™ assay was used to determine the time range of the toxic effects of the ILs. Using a continuous monitoring of cytotoxicity we were able to determine how soon after the addition of the ILs the first signs of toxicity appeared. For this assay we used HCE cells and treated them with the ILs at their EC_{50} concentrations for a maximum of 24 h, therefore, the maximum toxicity was expected to be 50%. Most ILs behaved in a similar manner, with moderate cell death apparent after a lag period of 8–10 h (Figure 3, Table 1). Noticeable exceptions were the long chained phosphonium ILs, [P_{14444}]Cl and [P_{14444}][OAc], which reached their maximum toxicity levels in less than 2 h of incubation.

Not all ILs could induce a 50% cell death measurable by the assay. The two assays for HCE cells (EC_{50} determination and real-time cytotoxicity assay) used to measure cell toxicity employ different methods of detection: the alamarBlue uses a membrane permeable dye and highlights the metabolic activity while the CellTox™ assay utilizes a non-permeant fluorescent dye that highlights cell breakage. This suggests that [P_{14444}]Cl and [P_{14444}][OAc] are the most efficient at destabilizing the plasma membrane. They affect significantly the integrity of the cellular membrane and the cells are lysed, while the other compounds induced cell death more slowly, showing a noticeable change in the cell viability after incubation of 24 hours. Using both methods, we obtained information about the cytotoxicity of ILs from different perspectives. For example, [N_{4441}][OAc] at its EC_{50} concentration kills 50% of the HCE cells by affecting the metabolism but the cell death is only 15% in the real-time cytotoxicity test after 24 hours,

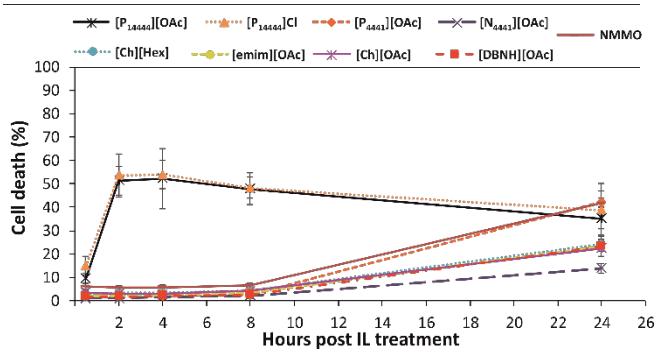

Figure 3. Real-time measurement of the cytotoxicity of ILs. HCE cells were treated with the compounds at the following concentrations: $[P_{14444}][OAc]$ 8 µM, $[P_{14444}]Cl$ 8 µM, $[P_{4441}][OAc]$ 12 mM, [emim][OAc] 46 mM, [Ch][OAc] 72 mM, [Ch][Hex] 15 mM, $[N_{4441}][OAc]$ 12 mM, [DBNH][OAc] 70 mM, and NMMO 270 mM. Data was collected at 2, 4, 8, and 24 hours post treatment.

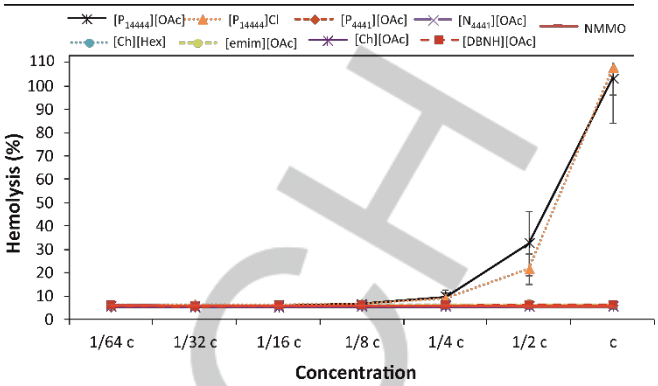

Figure 4. Hemolysis of red blood cells. Hemolysis was assessed using binary dilutions. Initial concentrations (c) were as follows: $[P_{14444}][OAc]$ 44 µM, $[P_{14444}]Cl$ 46 µM, $[P_{4441}][OAc]$ 45 mM, [emim][OAc] 147 mM, [Ch][OAc] 306 mM, [Ch][Hex] 228 mM, $[N_{4441}][OAc]$ 48 mM, [DBNH][OAc] 271 mM, and NMMO 850 mM. The red line indicates the negative control level of hemolysis.

indicating that the plasma membrane integrity is not significantly altered. On the other hand, for $[P_{4441}][OAc]$ a similar concentration affects equally the metabolism and the permeability of the plasma membrane. To assess the effect of ILs on the membrane breakage a red blood cell (RBC) hemolysis test was performed.

Hemolysis

The different mechanism of toxicity of the ILs was validated by a hemolysis assay, in which the ability of the ILs to lyse RBCs was tested (Figure 4, Table 1). Of all tested ILs only $[P_{14444}]Cl$ and $[P_{14444}][OAc]$ were able to lyse the RBCs. The lysis occurred when the IL concentrations exceeded their EC_{50} values. The hemolysis was tested at the same concentration ranges that were used for the EC_{50} calculation with the intention of understanding the most likely cause of cell death at the EC_{50} levels. In this particular assay the ILs were in contact with the cells for ca. 20 min, indicating that the time required for membrane perturbation is essential. IL-membrane interaction is time-dependent, as seen in Figure 3. However, it seems that prior to the time point when the compound penetration is initiated the compound concentration is insignificant, thus, the penetration is independent on the concentration. Figure 4 shows that ILs causing cell mortality after 24 hours (Figure 3) do not cause any effect on the RBCs within 20 min. For example, $[P_{4441}][OAc]$ could not induce cell lysis even at 45 mM - a concentration that is four times higher than the EC_{50} value. These experiments suggest that there is a clear difference between the mechanism of toxicity of the ILs, with $[P_{14444}]Cl$ and $[P_{14444}][OAc]$ affecting cell viability from the outside by disrupting the membrane integrity. In contrast, the other ILs require more time and/or their toxicity is most likely manifested intracellularly, affecting the cell metabolism. In order to gain more information on the mechanism of IL toxicity, several analytical methods were used for studying interactions between ILs and biomimicking liposomes.

Dynamic light scattering

Dynamic light scattering (DLS) was utilized to see if the ILs had an effect on the liposome size and zeta potential. The zeta potential describes the potential around the liposomes caused by the negatively charged phosphate groups of the lipids on the liposome surface. Figure 5 and Table 1 show that the sizes of the liposomes did not change remarkably upon addition of the ILs.

The effect of [emim][OAc], [Ch][OAc], and [DBNH][OAc] ILs on the zeta potential of the liposomes could not be determined at concentrations near and above their EC_{50} values due to high conductivity and, thus, oxidation of the electrodes. However, it seems that the zeta potential is not changing significantly at concentrations below the EC_{50} values. This indicates that the small IL cations are not adsorbed on the liposome surface, hence, not changing the surface charge (ca. -60 mV) of the liposomes. The same behavior was also seen with [Ch][Hex] and zwitterionic NMMO. [Ch][Hex] has a lipophilic component in the anion moiety causing an electrostatic repulsion between the hexanoate and liposome surface, and therefore possible sorption of the IL is not clearly observable with this technique. On the other hand, the effect caused by $[P_{4441}][OAc]$ and $[N_{4441}][OAc]$ on the liposomes was more substantial. These IL cations interact with the liposomes nearly neutralizing the liposome surface and resulting in only a slightly negative zeta potential. $[P_{4441}][OAc]$ decreased the zero potential more than $[N_{4441}][OAc]$ indicating a stronger interaction with the liposomes, seen in Figure 5. However, because the zeta potential was not converted from negative to positive, the cations seem to be loosely adsorbed on the surface of the liposomes and not penetrated into the membrane within the short incubation time used in this study.

The most toxic ILs, $[P_{14444}][OAc]$ and $[P_{14444}]Cl$, on the other hand, switched the zeta potential of the liposomes from negative to positive at a concentration of 0.015 mM, evidencing a strong, possibly irreversible, sorption of the ILs into/onto the liposome. The concentrations at which the zeta potentials turned positive were relatively close to the EC_{50} values (0.004-0.007 mM) of these ILs. In order to evaluate the compatibility of the results obtained using the two biomembrane sources (liposomes and HCE cells), the liposome amount and surface area as well as the concentration of lipids in HCE cells were estimated (SI page 3 and 4). The concentration of lipids used in the zeta potential measurements was 0.15 mM, which is equivalent to

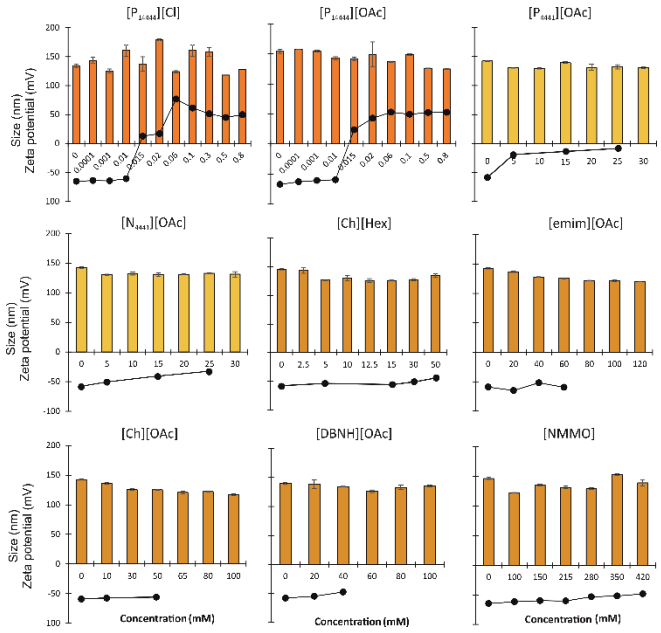

Figure 5. The effect of ILs and NMMO on size (z-average; marked as bars) and surface charge (zeta potential; marked as dots) of 0.15 mM eggPC/eggPG (80/20 mol%) liposomes.

approximately 300 billion liposomes, while the concentration of lipids in HCE cells was estimated to be 0.34 mM corresponding to 340 000 cells. Cells have bigger diameters than liposomes (8200 – 51 700 vs. 150 nm, respectively) hence, the surface area of liposomes, which is the first cellular constituent encountered of external toxicant, is also larger (15 000 vs. 67 – 2100 μm^2). However, because the concentrations and the surface areas of both biomembranes are in good agreement, the effect of toxicants were comparable and in a good agreement with each other.

It seems that the mechanism of toxicity of the $[P_{14444}]^+$ ILs is primarily related to a strong IL-biomembrane interaction of the cation: the same concentration of the IL caused a response of the biomembrane, *i.e.*, the IL penetrated into the membrane bilayer causing a cell mortality or conversion of the surface charge.

The sizes of the liposomes could not be measured reliably when the concentrations of $[P_{14444}]^+$ ILs exceeded 1 mM due to occurance of different sized IL-lipid aggregates (SI page 5) and overall the size distributions varied with time upon addition of $[P_{14444}]^+$ ILs. $[P_{14444}]^+$ cations seem to penetrate into the liposome, destabilizing the bilayer, and eventually rupturing the membrane and forming varying sized IL-lipid aggregates. This was already noticed in our previous study[7b] when L-*α*-phosphatidylcholine/ 1-palmitoyl-2-oleoyl-*sn*-glycero-3-phosphocholine (eggPC/POPG; 75/25 mol%) liposomes were used. However, in that work the breakage occurred already at 0.2 mM instead of 1 mM as seen in the current study. As seen from the real-time toxicity results, the incubation time of the sample has a noteworthy impact on the IL-cell interactions, and therefore we can assume that increasing the incubation time before the size measurement could have decreased the concentration rupturing the liposomes. To study the effect of ILs on the processes occurring inside the lipid bilayer, main phase transition temperature changes of dipalmitoylphosphatidylcholine (DPPC) liposomes were measured by differential scanning calorimetry (DSC).

Differential scanning calorimetry

DSC measures thermodynamic properties of phase transitions or conformational changes, which require or release energy. In liposomes, a phase transition occurs when a lipid bilayer undergoes a gradual transformation from an ordered gel phase into a disordered fluidic phase or vice versa within a short temperature range. When the lipid bilayer is perturbed with an external surface-active compound, the lipid order is reduced and its phase transition temperature is decreased. The effect of various concentrations of ILs and NMMO below and above their EC_{50} values on the DPPC phase transition temperature are shown in Figure 6 and summarized in Table 1.

In the case of [emim][OAc], [Ch][OAc], and [DBNH][OAc] the T_m of DPPC did not change at all, when concentrations six times higher than the EC_{50} were added to the lipid dispersion. This confirms that these ILs do not disturb at all the bilayer but, more likely, the small ILs passed through the membrane without compromising the ordered structure of the lipids in the bilayer. ILs are relatively small (<500-600 g/mol) and despite their charge they might be absorbed through the plasma membrane without causing any effect to the membrane itself (*transcellular permeability*). On the other hand, the smallest ILs (<150 g/mol) might also enter tissues via *paracellular permeability* using intercellular aqueducts for transportation or via suitable transporters. However, all ILs are charged and thus, it is plausible that they do not cross the plasma membrane at all but bind to receptors which induce subcellular responses inside the cell that elicit tissue dysfunction.[17] The external toxicant can be harmful itself or it can undergo metabolism and become toxic.[18] If the mechanism of toxicity is considered according to the hard-soft acid-base theory (HSAB theory)[19] the imidazolium and amidinium IL cations can be considered to be soft electrophiles, which prefer to interact with soft nucleophiles, *i.e.,* proteins, and can cause organ damage. Phosphonium and cholinium based IL, instead, can be considered as hard electrophiles and prefer to interact with DNA and RNA and are therefore prone to cause cancer. It has been suggested before that imidazolium based ILs can inhibit trypsin activity,[20] acetylcholinesterase enzymes,[21] and AMP deaminase activity[22], which supports the HSAB hypothesis. However, because of many possible IL combinations it is impossible to say what is the exact mechanism of toxicity of these ILs.

Instead of making the bilayer more disordered, zwitterionic NMMO seemed to stabilize the order of the lipids resulting in a slight increase of the T_m at concentrations above 200 mM. Interestingly [Ch][Hex], the only compound having a relatively long alkyl chain length in the anion, started to permeate into the liposome bilayer at concentration between 5 and 15 mM, causing the endotherm to shift to a lower temperature. The concentration corresponds to the EC_{50} value, meaning that the toxicity of

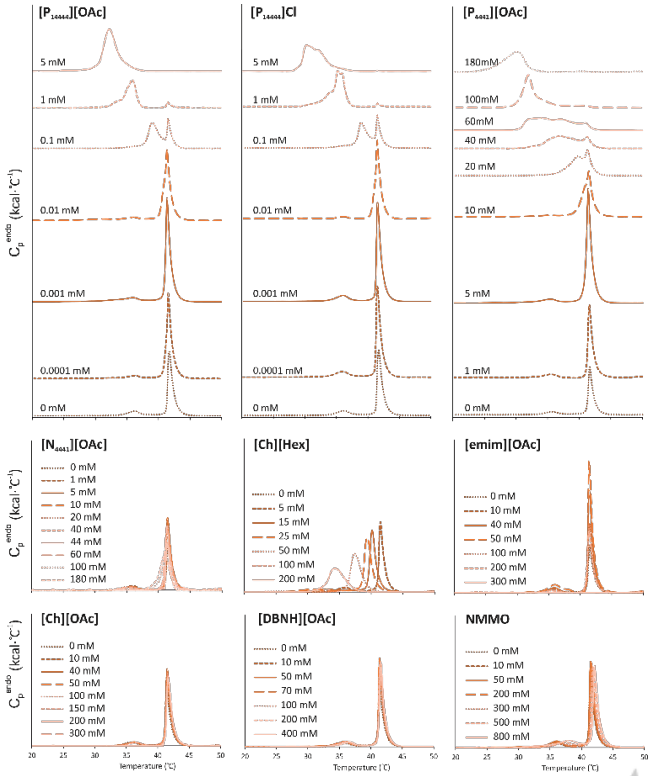

Figure 6. Effect of ILs and NMMO on the phase transition temperatures of 0.4 mM DPPC liposomes. Second endotherms are shown in the figure except the first endotherm is shown for $[P_{14444}]OAc$ and $[P_{14444}]Cl$ at concentration of 5 mM.

[Ch][Hex] is caused by the penetration of the IL into the bilayer, compromising the integrity of the plasma membrane, in addition of altering the organism metabolism as seen from the cytotoxicity assays.

$[N_{4441}][OAc]$ increased the zeta potential of the liposomes by adsorbing onto their surface. However, the DSC data show that the IL does not permeate into the bilayer at its EC_{50} concentration. The shift in the endotherm, at a concentration 10 times higher than the EC_{50}, is only minor, suggesting that the penetration is not extensive. This confirms that the mechanism of toxicity of $[N_{4441}][OAc]$ is an alteration in the metabolic activity of the cell and not related to the penetration of the IL into the plasma membrane. In contrast, the phosphonium based ILs $[P_{14444}][OAc]$, $[P_{14444}]Cl$, and $[P_{4441}][OAc]$ were able to permeate into the liposomes causing a decrease of the T_m. The effect of $[P_{4441}][OAc]$ was not as strong and immediate as with the longer chained ILs seen from the hemolysis test and from the zeta potential data. With all the phosphonium-based ILs the destabilization of the lipid bilayer occurred at concentrations in close proximity of their EC_{50} values. For $[P_{14444}][OAc]$ and $[P_{14444}]Cl$ at concentrations in the range of 0.001-0.01 mM (EC_{50} values are 0.007 and 0.004 mM, respectively) and for $[P_{4441}][OAc]$ at 5-10 mM (EC_{50} 10 mM). Therefore, it seems that the toxicity can be estimated utilizing DSC for these liposome permeating ILs, without the use of living organisms. An increase in the concentration decreased the T_m gradually and another endothermic peak appeared in the thermogram, proving an existence of two species in the system. Based on our earlier results[7c] we assume that the main endotherm corresponds to the pure lipid bilayer without a remarkable amount of surfactants included, and the second endotherm at a lower temperature corresponds to newly formed mixed lipid-surfactant vesicles or a heterogeneous lipid-surfactant area in the otherwise pure liposome. In our previous study[23] we have shown that the lamellar distances of 1-palmitoyl-2-oleyl-phosphatidylcholine (POPC) multilamellar vesicles (MLVs) decrease and the lamellar disorder increases when $[P_{14444}][OAc]$ was added to the dispersion. The IL at a concentration of 0.4 mM caused also uneven lamellar spacing in the MLVs, suggesting that the effect of the IL is possibly different on the outer and inner lamellae. Due to the fact that we used MLVs in the DSC studies instead of unilamellar vesicles, it is also possible that the heterogeneous outermost bilayer gives the signal at lower phase transition and the remains of the original signal at 41.3 °C is caused by the unaffected lipid lamellae close to the core of the liposome.

Lopez et al.[11] have shown that a gradual increase of Triton-X (a nonionic surfactant) concentration caused the surfactants to penetrate into the studied egg phosphatidylcholine liposome membrane until a saturation point was reached, followed by aggregation of surfactants and lipids, and a subsequent appearance of mixed vesicles and mixed micelles. This phenomenon is characteristic for lipids and surface-active compounds shown many times before.[24] The mixed micelles lack the ordered structure of a lipid bilayer and, thus, no phase transition takes place. It is plausible that during this process from pure liposomes to mixed vesicles and further to mixed micelles, a stage where heterogeneous vesicles with different sizes coexist. This was seen by DLS for $[P_{14444}]^+$; a wider size distribution was observed when the $[P_{14444}]^+$ concentration was increased, until a liposome breakage point was reached. The coexistence of mixed vesicles and mixed micelles is seen from the DSC scans as a decrease in the endothermic peak area upon increasing IL concentration. A constant concentration of 0.4 mM of DPPC liposomes was used in all measurements and all the thermograms were normalized to the DPPC concentration, omitting the impact of surfactant concentration. In order to normalize the needed energy for the phase transition to the amount of substance, the total concentration of unimers involved in the phase transition (all unimers in mixed vesicles) would have to be known. When the surfactant concentration is much below the DPPC concentration the impact of the normalization on the peak area is insignificant ($c[P_{14444}]^+$ ILs ≤ 0.1). However, at high concentrations ($c_{IL} >> c_{DPPC}$) the number of unimers in the vesicles ($c_{total\ unimers} - (c_{mixed\ micelles} + c_{free\ unimers})$) becomes significant and this might result in oversized peak areas. Yet, with all liposome penetrating ILs ($[P_{14444}][OAc]$, $[P_{14444}]Cl$, $[P_{4441}][OAc]$, and [Ch][Hex]) the peaks became smaller, proving that the number of bilayers undergoing phase transition is gradually decreasing. Moreover, when $[P_{14444}]^+$ ILs at a concentration of 5 mM were added to the liposome dispersion, only peaks in the first heat scans were observable (shown in Figure 6), whereas the second and third heat scans as well as all three cooling scans were flat. This indicates a total

disruption of the bilayer structure in the vesicles at the mentioned concentration.

From the DLS measurements we observed that there was more than one species (lipid and/or surfactant aggregate) existing when the concentration exceeded 1 mM. Therefore, it seems that $[P_{14444}]^+$ ILs initiate the permeation into the lipid bilayer at 0.001-0.1 mM concentration, gradually removing phospholipids from the liposomes when the IL concentration is further increased above 0.1 mM. It has been shown in our previous study[25] that at 1 mM $[P_{14444}][OAc]$ concentration the ILs are forming IL-lipid aggregates, yet the whole liposome integrity was not compromised. Raising the concentration of the ILs to 5 mM eventually irreversibly disrupt the remaining mixed vesicles and all the lipids and ILs are organized in aggregates without structures able to undergo phase transition at the temperature range used. However, it has been shown by Majhi et al. that a transition from mixed micelles to mixed vesicles can be detected at higher temperatures (40 to 70 °C) for a mixed surfactant/lipid system containing sodium dodecylsulfate and dimyristoyl phosphatidylcholine.[24c] In order to monitor the location of the IL unimers in the presence of liposomes pulsed field gradient (PFG) NMR was further utilized.

Nuclear magnetic resonance spectroscopy

As diffusion coefficients decrease upon aggregation of surfactants, PFG NMR is a valuable tool for CMC determinations, especially for CMC_1 and CMC_2 detection[26] as well as probing interactions between solution components. The diffusion coefficients of the IL cations and anions (Table 1) did not change significantly when $[N_{4441}][OAc]$, [DBNH][OAc], [emim][OAc], or [Ch][OAc] ILs were added to the LUV dispersions at any concentration compared to their diffusion coefficient in pure solvent. Interestingly, no significant change was observed even when mixing the membrane-interacting ILs $[P_{4441}][OAc]$ and [Ch][Hex] with the liposomes. It seems that the interactions of these ILs were too weak for detection with this technique. Furthermore, the neat ILs did not show changes in their diffusion coefficients, because the measurements were performed below the CMCs of the IL (CMCs are shown in Table 1). The diffusion coefficients of neat $[P_{14444}]Cl$ and $[P_{14444}][OAc]$ in D_2O decreased when the concentrations of the ILs increased from 0.8 to 5 mM (Figure 7), indicating an aggregation of the cations. The most abrupt change was observed at 1.2 mM (CMC_1), which correlates with the CMC values previously determined by our group (0.9 mM for $[P_{14444}][OAc]$[13] and 1 mM for the $[P_{14444}]Cl$[7b] in water) by surface tension measurements. We have earlier confirmed that the aggregation of $[P_{14444}]^+$ occurs in a narrow concentration range. Therefore, the observed NMR diffusion coefficient above the CMC was considered as the diffusion coefficient of the sole aggregate, even though the fast exchange kinetics between the free and aggregated ILs and the longer timescale of the NMR experiment may lead to a signal averaged from both species.[26-27] Above the CMC_1, the diffusion coefficients kept decreasing upon increasing concentration of ILs, indicating a continuation of aggregation. One plausible explanation is that $[P_{14444}]^+$ ILs initially form micelles around their CMC due to their long alkyl chains and they are then able to aggregate further when the concentration is increased. However, a clear breaking point was absent and a value representing a CMC_2 above 1.2 mM concentration could not be determined. Using the Stokes-Einstein equation (equation 2) estimations of the sizes of diffusing species were done: the size of $[P_{14444}]^+$ below the CMC_1 value (<1.2 mM) varies between 1.3 – 1.4 nm. The size of a single $[P_{14444}]^+$ molecule using a simple 3D model yields a largest distance of 2.3 nm, assuming that the angles between the carbon bonds in the alkyl chains are constant (109.5°). However, the hydrophobic chains of the molecules are not fully extended in water solution, and therefore the size of an average molecule correlates well with the experimentally observed size from PFG NMR measurements. The results show that the size of the IL aggregates increases to 2.1 nm above the CMC_1 (1.2 – 2 mM), indicating aggregation of the ILs. When exceeding 2 mM IL concentration the aggregate size increases further to 3.5–3.8 nm, evidencing the formation of larger aggregates.

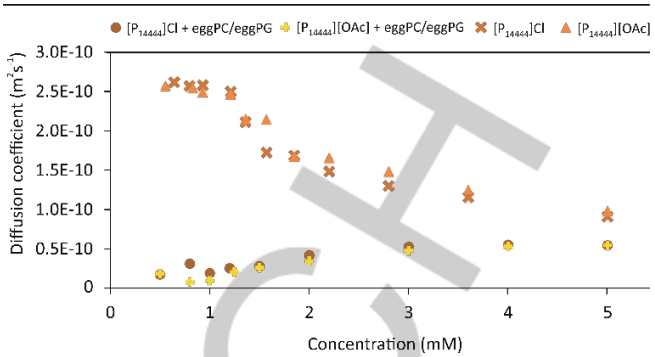

Figure 7. Diffusion coefficients of $[P_{14444}][OAc]$ and $[P_{14444}]Cl$ with and without the presence of 1 mM eggPC/eggPG (80/20 mol%) liposomes.

The diffusion coefficient of pure liposomes was approximately $3 \cdot 10^{-12}$ $m^2 s^{-1}$, which corresponds to a size of 120 nm and agrees well with the DLS data. When $[P_{14444}][OAc]$ and $[P_{14444}]Cl$ were introduced to the liposome dispersion, the diffusion coefficients of the ILs were over eight times smaller than in the absence of liposomes, Figure 7. This is a clear indication that these ILs interact with the liposomes making them diffuse slower. The diffusion coefficients of the ILs started to increase above 1 mM concentration, showing that some of the ILs were disengaged from the liposomes. Because, neat IL molecules are known to aggregate at 1 mM concentration (cmcs for $[P_{14444}][OAc]$ and $[P_{14444}]Cl$ are 0.9 and 1.0 mM, respectively; Table 1) it is not likely that free unimers occur above 1 mM concentration. DSC measurements show that $[P_{14444}]^+$ ILs disrupt liposomes, thus, it is likely that the ILs aggregate with the disrupted lipids forming IL-lipid aggregates. It has previously been shown that amphiphilic long alkyl chained imidazolium based ILs rupture liposomes, resulting in the formation of IL-lipid micelles in aqueous suspensions.[8c] Above 2 mM concentration, the diffusion coefficients increased but did not reach the values of the neat IL micelles, indicating a balance between the smaller IL aggregates and bigger IL-lipid aggregates.

Conclusions

Toxicities of a set of ionic liquids with different surface-active properties were evaluated using two different cell lines and correlated to changes observed by DLS, DSC, and NMR. All ILs were more toxic towards *V. fischeri* bacteria than towards HCE cells. This is assumed to be due to a different detection method or/and due to a different cell structure and metabolism. The toxicity was shown to be highly dependent on time. While long alkyl chained phosphonium ILs ([P_{14444}][OAc] and [P_{14444}]Cl) exerted toxicity within 2 hours post treatment, it took 24 hours to see the same response with the other studied compounds ([P_{4441}][OAc], [N_{4441}][OAc], [Ch][Hex], [emim][OAc], [Ch][OAc], [DBNH][OAc], and NMMO). In addition, it was shown that within a short period of time (20 min) only [P_{14444}][OAc] and [P_{14444}]Cl could induce cell lysis, even at concentrations 3 to 14 times higher than the EC_{50} values. [P_{4441}][OAc] and [Ch][Hex] were shown to permeate the cell membrane, however, hemolysis did not take place. This indicates that the cell lysis is independent on the toxicant concentration prior to the threshold time point at which the cell penetration is initiated. In addition, the time and concentration dependencies are determined by the IL structure and the mechanism of toxicity.

According to DLS, the liposome sizes did not change remarkably upon addition of [P_{4441}][OAc], [N_{4441}][OAc], [Ch][Hex], [emim][OAc], [Ch][OAc], [DBNH][OAc], or NMMO. For [P_{14444}][OAc] and [P_{14444}]Cl the sizes were relatively stable prior to the liposome breakage point, whereas multiple aggregate sizes appeared after the liposomes had ruptured. Changes in the zeta potential of the liposomes were negligible for [Ch][Hex], [emim][OAc], [Ch][OAc], [DBNH][OAc], and NMMO, whereas the values increased for [P_{4441}][OAc], [N_{4441}][OAc] but remained negative. However, upon addition of [P_{14444}][OAc] and [P_{14444}]Cl positive zeta potential values were observed above 0.01 mM IL concentration. This indicates that the long alkyl chain ILs have permanent irreversible interactions with the liposomes while the other compounds have lesser or no interactions at all with the membranes. DSC data revealed that in addition to [P_{14444}][OAc] and [P_{14444}]Cl ILs, also [P_{4441}][OAc] and [Ch][Hex] penetrate into the liposome membranes. The membrane penetration is initiated at concentrations equivalent to the EC_{50} values. NMR data verified that [P_{14444}][OAc] and [P_{14444}]Cl were the only ILs having resilient interactions with the studied liposomes. In addition, the formation of novel IL-lipid micelles after liposome breakage was observed. The results show that the cytotoxicity of ILs is highly dependent on the used cell line and the time of the IL exposure. When the time of the effect (threshold) is exceeded, the toxicity is also dependent on the concentration. Furthermore, the dependency itself is determined by the IL structure. Based on the data shown in this study, we can divide the ILs into three categories: cell membrane rupturing ILs ([P_{14444}][OAc] and [P_{14444}]Cl,) partially cell membrane rupturing ILs ([P_{4441}][OAc] and [Ch][Hex]), and compounds that affect the cell metabolism ([N_{4441}][OAc], [emim][OAc], [Ch][OAc], [DBNH][OAc], and NMMO).

Experimental Section

Chemicals

All the lipid stocks eggPC (Egg, Chicken) L-α-phosphatidylglycerol (eggPG; Egg, Chicken; sodium salt), and DPPC in chloroform were purchased from Avanti Polar Lipids (Alabaster, Alabama, USA). Deuterated water (99.9%), used for all IL and IL-liposome dilutions in NMR measurements was purchased from Euriso-Top (France). Methanol was from Sigma (Steinheim, Germany).

Cells

HCE are epithelial cells that occupy the outermost layer of cornea and grow as adherent monolayers in cultures. They represent a well defined cell line for drug toxicity studies.[28] Ham's F12/Dulbecco's modified eagle medium (DMEM), fetal bovine serum (FBS), human epidermal growth factor (EGF), insulin, gentamicin, alamarBlue, and cell culture ware were purchased from Thermo Fischer Scientific (Grand Island, NY). Cholera toxin was purchased from Sigma-Aldrich-Merck (St. Louis, MO). *V. fischeri* marine bacteria, reconstitution solution, and osmotic adjustment solution for running the Microtox assay were purchased form Modern Water (New Castle, DE, USA).

Ionic liquids

[emim][OAc] was purchased from IoLiTec GmbH (Heilbronn, Germany) and NMMO was from Sigma (Schnelldorf, Germany). [P_{14444}]Cl was provided by Cytec Industries (Woodland Park, NJ). Synthesis and characterization of [Ch][OAc], [Ch][Hex], and [N_{4441}][OAc] are shown in SI (Pages S6-S8). [DBNH][OAc] was synthesized according to a previously published method.[29] [P_{14444}][OAc] was synthesized by anion metathesis described in previous articles[7b,30] and HCE[P_{4441}][OAc] was synthesized from tributylmethylphosphonium methyl carbonate according to our previous article.[13]

Liposome preparation

Phosphatidylcholine is the main component of the cell membrane and therefore eggPC was used as a main lipid for preparing the biomimicking liposomes. In order to gain a negative surface charge, naturally occurring in eukaryotic cells, 20 mol% of eggPG was added to the lipid dispersion. The lipid stocks in chloroform were mixed in suitable proportions and chloroform was evaporated using air. The lipid film was further dried under reduced pressure over night to ensure the removal of chloroform traces. Next, the lipids were suspended in water by heating the dispersion at 60 °C for 1 hour in a thermoshaker. Finally, the lipid MLV dispersion was extruded 19 times through a 100 nm polycarbonate membrane in order to obtain large unilamellar vesicles. Instead of eggPC, multilamellar DPPC was used in DSC studies. DPPC has a well-defined phase transition temperature at 41.3 °C,[31] whereas the phase transition of eggPC occurs in a wider temperature region due to its high content of different fatty acid moieties with a varying degree of saturated chains.[32] Therefore, a temperature range of 10–60 °C was applied in the DSC studies.

Cytotoxicity assays

Vibrio fischeri

Microtox® M500 luminometer/thermostate (Modern Water, USA) was used to measure the EC_{50} values for the ILs using bioluminescencing *V. fischeri* marine bacteria. The instructions of the manufacturer for aqueous samples were followed. In short, bioluminescence was measured before and after the exposure to at least four IL dilutions and the decay in the bioluminescence of the bacteria was recorded. The EC_{50} values were determined after 5 and 15 minutes post IL treatment using the Modern Water MicrotoxOmni 4.2 software. Measurements were performed for each IL at least two individual times as duplicates and the error bars are given as standard deviations.

Human corneal epithelial cells

An alamarBlue assay (Invitrogen) was used as a fluorometric/colorimetric cell viability indicator to determine the EC_{50} values of the ILs. The alamarBlue reagent is reduced from a non-fluorescent state (blue) to a fluorescent state (red) in the presence of metabolically active cells (live cells). The SV-40 immortalized HCE cells[33] were grown in 48-well plates in a cell culture mixture containing DMEM/Ham's F12 medium supplemented with 15% FBS, 5 $\mu g \cdot mL^{-1}$ insulin, 10 $ng \cdot mL^{-1}$ human EGF, 1 $\mu g \cdot mL^{-1}$ glutamine, 0.1 $\mu g \cdot mL^{-1}$ cholera toxin, and 40 $\mu g \cdot mL^{-1}$ gentamycin. After confluence, they were serum-starved over-night. The serum-starved cells were incubated in serum-free medium at 37°C in atmosphere containing 5% CO_2 for 24 h. Each plate contained at least 7 different IL concentrations as triplicates. AlamarBlue solution was added to every well (1:10 v:v) 90 min before the incubation time expired. An aliquot of each well was transferred to a black 96-well plate and fluorescence was determined with a multimodal plate reader (EnSpire – PerkinElmer, Waltham, MA) at excitation/emission wavelengths of 570/590 nm. Cells incubated with media and dye were used as a positive control and media with dye was used as a blank sample on each plate.

In order to determine the correlation between the number of cells and fluorescence a calibration curve was prepared. A dilution series of the cells was made in serum free media and the fluorescence was determined after 90 minutes incubation with alamarBlue. The number of cells in the IL treated samples were calculated from a second order polynomial equation obtained from the calibration curve and the values were normalized to the positive control. Finally, a logistic sigmoid function was applied to determine the EC_{50} values for each IL. All measurements were repeated three times and the error bars were given as standard deviations.

Real-time cytotoxicity assay

CellTox™ Green cytotoxicity assay (Promega, Madison, WI) was used to determine the time line of the IL-induced changes in the membrane integrity of the HCE cells. The assay uses a cyanine dye that is not attached to viable cells but stains the DNA strands of the dead cells once the integrity of the plasma membrane has been compromised. Upon binding to DNA from non-viable cells, the dye becomes fluorescent, and the fluorescence is directly proportional to the level of cell death. By adding the dye in the cell culture media together with the IL we were able to monitor the changes in fluorescence/cell viability in real time and construct a kinetic curve of IL cytotoxicity. The HCE cells were seeded on a 96-well plate at 20 000 cells/well and allowed to attach for two hours. The ILs were dissolved in the cell culture media at concentrations in close proximity to their EC_{50} values and they were added to the attached cells together with the CellTox™ Green dye. Changes in the fluorescence signal were measured after 30 min, 2 h, 4 h, 8 h, and 24 h by reading the plate at excitation/emission wavelengths of 485/520 nm. Cells incubated with media and dye were used as a negative control. Cells lysed with the lysis solution, provided with the kit, were considered as the positive control and determined the upper limit of the fluorescence reading (100% cell death reached). In order to calculate the number of dead cells at each time point, a scale of cytotoxicity was created by mixing live and dead cells in determined proportions. For this, the cells were divided in two, and one half was kept untouched, while the other half was sonicated to simulate a 100% dead population of the cells. These two populations of cells were then mixed in different proportions to cover the entire scale of toxicity – from 0% to 100% dead cells. A second order polynomial function was used to link the fluorescence units to the number of cells. Each plate contained three repetitions of each IL concentration and the experiments were repeated twice. The error bars are standard deviations.

Red blood cell hemolysis

The capacity of the ILs to induce cell lysis was measured using RBCs in a hemolysis assay.[34] Blood collected in dipotassium ethylenediaminetetraacetic acid (K_2EDTA) spray-coated tubes was centrifuged (750 g) at room temperature for 5 min and plasma was discarded. The resultant RBC pellet was re-suspended in isotonic phosphate buffer (pH 7.4, PBS), and centrifuged three more times. The washed RBC pellet was diluted with PBS 3:11 (v/v) to constitute the RBC stock dispersion. The IL dilution series containing 8 different concentrations below and above the EC_{50} values, were prepared in PBS and mixed with the RBC stock dispersion 1:10 (v:v). All samples and controls were incubated for 5 min at room temperature with shaking and centrifuged at 3000 rpm for 3 min to pellet unbroken RBC. 25 µL of the resultant supernatant was mixed with 500 µL of 99.7% ethanol and 37% HCl mixture (39:1; v/v) and the absorbance was measured with a multimodal plate reader at 398 nm. 100% hemolysis was obtained by mixing the RBC stock dispersion with distilled water 1:10 (v:v) and PBS alone was used as a negative control. The relative hemolysis was calculated as A_{398}sample/A_{398}positive control × 100%, where A_{398} represents the absorbance measured at 398 nm. Each sample was run in triplicate or as quadruplicate and the error bars were calculated as standard deviations.

Dynamic light scattering

DLS measurements were performed using a Malvern Zetasizer Nano ZS (Malvern Instruments Ltd, Worcestershire, UK) in order to determine the effect of the ILs on the size and zeta potential (surface charge) of unilamellar eggPC/eggPG (80/20 mol%) liposomes in water. Size and zeta potential determinations were performed employing a helium/neon laser at 633 nm and using

laser Doppler micro-electrophoresis, respectively. The liposome dispersion concentration was kept constant at 0.15 mM and IL concentrations were chosen to vary below and above their EC_{50} values. All measurements were conducted at constant temperature of 20 ˚C using disposable cuvettes and disposable folded capillary cells for size and zeta potential measurements, respectively. All samples were measured three times – one run consisting of a minimum of ten individual measurements and the error bars were calculated as standard deviations. The ILs were mixed with liposomes 10–15 minutes before each measurement.

Differential scanning calorimetry

Microcalorimetry (DSC) measurements were conducted with a VP-DSC MicroCalorimeter (MicroCal LLC, MA, USA) to determine the effect of ILs on the main phase transition temperature (T_m) of DPPC liposomes. A heating rate of 60 ˚C·h^{-1} was used within a temperature range from 10 to 60 ˚C. Multilamellar DPPC liposome dispersions (0.4 mM) with and without ILs were degassed under vacuum for ca. 5 min prior to the DSC measurements. The concentrations of the ILs varied below and above their EC_{50} values and all samples were diluted in Milli-Q water. Three heating and three cooling scans were recorded and the samples were kept at 10 ˚C for 30 min prior to the heating scans.

Nuclear magnetic resonance spectroscopy

^{1}H and PFG NMR measurements were performed on a 500 MHz Bruker Avance III spectrometer equipped with a 5 mm BBFO probe with Z-axis gradient. All PFG NMR measurements were conducted on ^{1}H nuclei with diffusion ordered spectroscopy (DOSY) using a stimulated echo pulse sequence (longitudinal eddy delay and bipolar gradient pulses). The gradient strength (G) of the pulses varied from 2 to 95% of the maximum gradient strength (0.47 T·m^{-1}) in 32 steps. The durations of the gradient pulses (δ, 2 ms), the delay time (Δ, 150 ms), and the temperature (T, 21 ˚C) were kept constant. The signal attenuation (S) of probe molecules with gradient strength variation were recorded and analyzed using Top Spin software to extract the translational diffusion coefficients (D). When probe molecules are in unhindered motion, the signal is attenuated with respect to the signal in the absence of a gradient (S_0) as

$$\frac{I}{I_0} = \exp\left(-\gamma^2\delta^2G^2D\left(\Delta - \frac{\delta}{3}\right)\right) \quad (1)$$

where the gyromagnetic ratio (γ) is 42.6 MHz·T^{-1} for ^{1}H nuclei. Furthermore, the hydrodynamic radius (R_h) of the diffusing aggregates were estimated from the Stokes-Einstein equation

$$D = \frac{k_BT}{6\pi\eta R_h} \quad (2)$$

where k_B is the Boltzmann constant, T is the temperature, and η is the viscosity.

Critical micelle concentration determinations

The critical micelle concentration (CMC) determinations of [Ch][Hex] and [N_{4441}][OAc] in water were performed using a contact angle meter (CAM 200 Optical Contact Angle Meter, Biolin Scientific, KSV Instruments, Finland) measuring the surface tension of a drop upon an increasing concentration of the IL (optical pendant drop method). The method is described in more detailed in our previous articles.[7b,35]

Acknowledgements

Financial support from the Academy of Finland (project number 266342 SKW) and Magnus Ehrnrooth foundation (project number 4703943) are greatly acknowledged. Harry Ahlgren, Ganesh Poudel, Jesper Långbacka, and Jean-Paul Heeb are acknowledged for their assistance with the DSC, DLS, and NMR measurements.

Keywords: analytical methods • cytotoxicity • ionic liquids • liposomes • toxicology

[1] K. S. Egorova, E. G. Gordeev, V. P. Ananikov, *Chem. Rev.* **2017**, *117*, 7132-7189.

[2] M. Amde, J.-F. Liu, L. Pang, *Environ. Sci. Technol.* **2015**, *49*, 12611-12627.

[3] A. A. Toledo Hijo, G. J. Maximo, M. C. Costa, E. A. Batista, A. J. Meirelles, *ACS Sustain. Chem. Eng.* **2016**, *4*, 5347-5369.

[4] Z. S. Qureshi, K. M. Deshmukh, B. M. Bhanage, *Clean Technol. Environ. Policy* **2014**, *16*, 1487-1513.

[5] P. Sun, D. W. Armstrong, *Anal. Chim. Acta* **2010**, *661*, 1-16.

[6] a) K. S. Egorova, V. P. Ananikov, *ChemSusChem* **2014**, *7*, 336-360; b) T. P. Thuy Pham, C.-W. Cho, Y.-S. Yun, *Water Res.* **2010**, *44*, 352-372; c) D. Zhao, Y. Liao, Z. Zhang, *CLEAN–Soil, Air, Water* **2007**, *35*, 42-48; d) M. Cvjetko Bubalo, K. Radošević, I. Radojčić Redovniković, J. Halambek, V. Gaurina Srček, *Ecotox. Environ. Safe.* **2014**, *99*, 1-12; e) S. P. Costa, A. M. Azevedo, P. C. Pinto, M. Saraiva, *ChemSusChem* **2017**, *10*, 2321-2347.

[7] a) P. Galletti, D. Malferrari, C. Samori, G. Sartor, E. Tagliavini, *Colloid Surf. B-Biointerfaces* **2015**, *125*, 142-150; b) S.-K. Mikkola, A. Robciuc, J. Lokajová, A. J. Holding, M. Lämmerhofer, I. Kilpeläinen, J. M. Holopainen, A. W. T. King, S. K. Wiedmer, *Environ. Sci. Technol.* **2015**, *49*, 1870-1878; c) A. H. Rantamäki, S.-K. Ruokonen, E. Sklavounos, L. Kyllönen, A. W. King, S. K. Wiedmer, *Sci. Rep.* **2017**, *7*, 1-12; d) K. O. Evans, *Colloid Surf. A-Physicochem. Eng. Asp.* **2006**, *274*, 11-17.

[8] a) N. Gal, D. Malferarri, S. Kolusheva, P. Galletti, E. Tagliavini, R. Jelinek, *Biochim. Biophys. Acta-Biomembr.* **2012**, *1818*, 2967–2974; b) J. Ranke, A. Muller, U. Bottin-Weber, F. Stock, S. Stolte, J. Arning, R. Stormann, B. Jastorff, *Ecotox. Environ. Safe.* **2007**, *67*, 430-438; c) B. Jing, N. Lan, J. Qiu, Y. Zhu, *J. Phys. Chem. B* **2016**, *120*, 2781-2789; d) M. Galluzzi, S. W. Zhang, S. Mohamadi, A. Vakurov, A. Podesta, A. Nelson, *Langmuir* **2013**, *29*, 6573-6581.

[9] M. Matzke, J. Arning, J. Ranke, B. Jastorff, S. Stolte, in *Handbook of Green Chemistry*, Bremen, Germany, **2010**, pp. 233–298.

[10] B. Yoo, J. K. Shah, Y. Zhu, E. J. Maginn, *Soft Matter* **2014**, 8641-8651.

[11] O. Lopez, A. de la Maza, L. Coderch, C. Lopez-Iglesias, E. Wehrli, J. L. Parra, *FEBS Lett.* **1998**, *426*, 314-318.

[12] E. H. Hayakawa, E. Mochizuki, T. Tsuda, K. Akiyoshi, H. Matsuoka, S. Kuwabata, *Plos One* **2013**, *8*, e85467.

[13] S.-K. Ruokonen, C. Sanwald, M. Sundvik, S. Polnick, K. Vyavaharkar, F. Duša, A. J. Holding, A. W. T. King, I. A. Kilpeläinen, M. Lämmerhofer, P. Panula, S. K. Wiedmer, *Environ. Sci. Technol.* **2016**, *50*, 7116-7125.

[14] B. Lachance, P. Y. Robidoux, J. Hawari, G. Ampleman, S. Thiboutot, G. I. Sunahara, *Mutat. Res. Genet. Toxicol. Environ. Mutagen.* **1999**, *444*, 25-39.
[15] N. S. Kudryasheva, *J. Photochem. Photobiol. B-Biol.* **2006**, *83*, 77-86.
[16] A. Mariscal, M. T. Peinado, M. Carnero-Varo, J. Fernández-Crehuet, *Chemosphere* **2003**, *50*, 349-354.
[17] a) A. P. Li, *Current Topics in Medicinal Chemistry* **2004**, *4*, 701-706; b) P. C. Burcham, *An introduction to toxicology*, Springer, **2013**.
[18] D. C. Liebler, F. P. Guengerich, *Nature reviews Drug discovery* **2005**, *4*, 410-420.
[19] R. M. LoPachin, T. Gavin, A. DeCaprio, D. S. Barber, *Chem. Res. Toxicol.* **2011**, *25*, 239-251.
[20] Y. Fan, X. Dong, L. Yan, D. Li, S. Hua, C. Hu, C. Pan, *Chemosphere* **2016**, *148*, 241-247.
[21] F. Stock, J. Hoffmann, J. Ranke, R. Störmann, B. Ondruschka, B. Jastorff, *Green Chem.* **2004**, *6*, 286-290.
[22] A. Składanowski, P. Stepnowski, K. Kleszczyński, B. Dmochowska, *Environ. Toxicol. Pharmacol.* **2005**, *19*, 291-296.
[23] I. Kontro, K. Svedström, F. Duša, P. Ahvenainen, S.-K. Ruokonen, J. Witos, S. K. Wiedmer, *Chem. Phys. Lipids* **2016**, *201*, 59-66.
[24] a) D. Lichtenberg, H. Ahyayauch, A. Alonso, F. M. Goni, *Trends Biochem. Sci.* **2013**, *38*, 85-93; b) H. Heerklotz, *Q. Rev. Biophys.* **2008**, *41*, 205-264; c) P. R. Majhi, A. Blume, *J. Phys. Chem. B* **2002**, *106*, 10753-10763.
[25] J. Witos, G. Russo, S.-K. Ruokonen, S. K. Wiedmer, *Langmuir* **2017**, *33*, 1066-1076.
[26] M. Figueira-González, V. Francisco, L. García-Río, E. F. Marques, M. Parajó, P. Rodríguez-Dafonte, *J. Phys. Chem. B* **2013**, *117*, 2926-2937.
[27] A. Cornellas, L. Perez, F. Comelles, I. Ribosa, A. Manresa, M. T. Garcia, *J. Colloid Interface Sci.* **2011**, *355*, 164-171.
[28] S. Rönkkö, K.-S. Vellonen, K. Järvinen, E. Toropainen, A. Urtti, *Drug Deliv. Transl. Res.* **2016**, *6*, 660-675.
[29] A. Parviainen, A. W. T. King, I. Mutikainen, M. Hummel, C. Selg, L. K. J. Hauru, H. Sixta, I. Kilpeläinen, *ChemSusChem* **2013**, *6*, 2161-2169.
[30] A. J. Holding, M. Heikkilä, I. Kilpeläinen, A. W. T. King, *ChemSusChem* **2014**, *7*, 1422-1434.
[31] M. H. Chiu, E. J. Prenner, *J. Pharm. Bioallied Sci.* **2011**, *3*, 39.
[32] F. R. S. Atta-ur-Rahman, *Studies in Natural Products Chemistry, Vol. 34*, Elsevier Science, Pakistan, **2008**.
[33] K. Araki-Sasaki, Y. Ohashi, T. Sasabe, K. Hayashi, H. Watanabe, Y. Tano, H. Handa, *Invest. Ophthalmol. Vis. Sci.* **1995**, *36*, 614-621.
[34] O. Reer, T. K. Bock, B. W. Müller, *J. Pharm. Sci.* **1994**, *83*, 1345-1349.
[35] F. Duša, S.-K. Ruokonen, J. Petrovaj, T. Viitala, S. K. Wiedmer, *Colloid Surf. B: Biointerfaces* **2015**, *136*, 496-505.

Entry for the Table of Contents (Please choose one layout)

Layout 1:

FULL PAPER

Make it simple: The toxicity of ionic liquids is predicted using biomimicking liposomes instead of living organisms and the results are in a good agreement with the cytotoxicity results obtained using various cell lines.

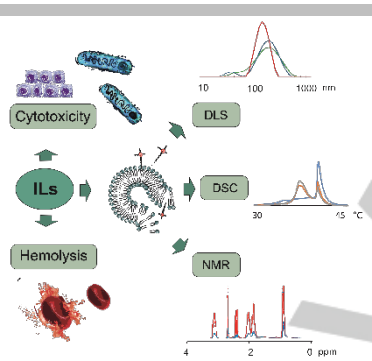

*Author(s), Corresponding Author(s)**

Page No. – Page No.

Title